J Math Chem (2012) 50:410–420
DOI 10.1007/s10910-011-9936-y

ORIGINAL PAPER

Detecting point sources in CMB maps using an efficient parallel algorithm

P. Alonso · F. Argüeso · R. Cortina · J. Ranilla · A. M. Vidal

Received: 14 September 2011 / Accepted: 20 October 2011 / Published online: 3 November 2011

Abstract The Cosmic Microwave Background (CMB) is a diffuse radiation which is contaminated by the radiation emitted by point sources. The precise knowledge of CMB fluctuations can lead to a better knowledge of the chemistry at the early stages of the Universe. In this work, we present an efficient algorithm, with a high degree of parallelism, which can improve, from the computational point of view, the classical approaches for detecting point sources in Cosmic Microwave Background maps. High performance computing libraries and parallel computing techniques have allowed to construct a portable, fast and numerically stable algorithm. To check the performance of the new method, we have carried out several simulations resembling the observational data collected by the Low Frequency Instrument of the Planck satellite. The sources are detected in their real positions.

Keywords Cosmic microwave background · Efficiency · Parallel algorithm

1 Introduction

In its early stages, after the nucleosynthesis epoch, the Universe can be considered as a plasma formed by ions and electrons[1] which interact with the radiation through

[1] There is also dark matter which only interacts gravitationally with the radiation.

P. Alonso (✉) · F. Argüeso
Department of Mathematics, University of Oviedo, 33203 Gijón, Spain
e-mail: palonso@uniovi.es

R. Cortina · J. Ranilla
Department of Computer Science, University of Oviedo, 33203 Gijón, Spain

A. M. Vidal
Department of Information Systems and Computation, Universidad Politécnica de Valencia, 46022 Valencia, Spain

scattering processes. When the Universe is about 380,000 years old, this plasma cools down due to its expansion to low enough temperatures for the formation of atoms to take place. Then, the first atoms, basically hydrogen and helium, are formed. This process gives rise to the decoupling between radiation and matter and from that moment on, the radiation propagates freely. This relic radiation is what we call the Cosmic Microwave Background (CMB).

Thus, the CMB is a diffuse radiation which comes from the beginning of the Universe, carrying relevant information about its origin, evolution and structure. Since its discovery in 1964 by Penzias and Wilson (see [17]), the CMB has been measured by instruments aboard balloons and satellites such as the NASA COBE satellite (1992) ([19]), which detected the CMB fluctuations, i. e. spatial variations of the CMB temperature on the celestial sphere, for the first time. In 2003, another NASA satellite, WMAP, used these fluctuations to determine the cosmological parameters with unprecedented accuracy (see [20]). In 2009, the ESA Planck satellite was launched and nowadays it is gathering CMB data in order to improve the knowledge about our Universe (see [1,21]).

There has been a great interest (see for instance [11,15,18]) in studying the effect of primordial chemistry on the CMB fluctuations. Line absorption, photoionization and photodissociation leave their imprint on the CMB power spectrum. A precise detection of the CMB fluctuations is essential to analyze these phenomena and to put constraints on the proportion of different molecules in the early Universe.

The CMB is contaminated by the radiation emitted by point sources, i. e. galaxies. The detection of these point sources is vital for cleaning the radiation maps and also from the astrophysical point of view (see [14,22]). The removal of point sources after their detection allows a more precise analysis of the CMB fluctuations. The precise knowledge of these fluctuations can lead to a better knowledge of the chemistry at the early stages of the Universe.

In [5] a method for detecting point sources in CMB maps was presented. [5] uses the Neville elimination, which has some computational advantages when working with positive matrices, sign-regular matrices or other related types of matrices (see, for example, [2–4,12]). However, this approach does not consider the structure of the input matrix of CMB maps. These matrices are Toeplitz-block Toeplitz (see [23]). Using the features provided for the structure of this kind of matrices it is possible to obtain an efficient algorithm that reduces the computational cost of the algorithm presented in [5].

Consequently, in this paper we present a new approach for detecting and removing point sources in CMB maps. Even though they share the goal they are quite different, the new method is computationally more efficient and uses standard strategies based on the structure of the matrices to solve the problem (without resorting to Neville elimination). The new method is applied to the detection of point sources in simulated CMB maps. We carry out simulations which have the characteristics of the Low Frequency Instrument (LFI) of the Planck satellite. These simulations show that the new method performs very well at detecting point sources in the simulated maps.

It is worth to highlight that mathematical and computational methods presented in this work can be applied to solve efficiently a large class of chemistry problems. The solution of the matrix equation and calculation of the matrix inverse of

a square matrix are recurrent tasks handled by molecular modeling software (see [9]). Moreover, in Quantum Chemistry, inversion of the overlap matrix between basis functions is required to obtain the electronic energy and to perform charge density analysis. Hence, the availability of more efficient direct methods for solving matrix equations could be of particular interest.

The paper is organized as follows. In Sect. 2 we will present the problem description. An efficient algorithm for solving the problem described is presented in Sect. 3. Finally, in Sects. 4 and 5 we describe the implementation details, the experimental results achieved and the simulations carried out to check the goodness of the method.

2 Problem description

In this section we will present a typical method of point source detection in CMB maps.

In a region of the celestial sphere, we suppose to have a certain number n of radio sources that can be considered as point-like objects if compared to the angular resolution of our instruments. This means that their actual size is smaller than our smallest resolution cell. The emission of these sources is superimposed to the radiation $f(x, y)$. In our particular case this radiation is the CMB. A model for the emission as a function of the position (x, y) is:

$$\tilde{d}(x, y) = f(x, y) + \sum_{\alpha=1}^{n} a_\alpha \, \delta(x - x_\alpha, y - y_\alpha)$$

where $\delta(x, y)$ is the 2D Dirac delta function, the pairs are the locations of the point sources in our region of the celestial sphere, and a_α are their intensities. We observe this radiation through an instrument, with beam pattern $b(x, y)$, and a sensor that adds a random noise $n(x, y)$ to the signal measured. Again, as a function of the position, the output of our instrument is:

$$d(x, y) = \sum_{\alpha=1}^{n} a_\alpha \, b(x - x_\alpha, y - y_\alpha) + (f * b)(x, y) + n(x, y) \tag{1}$$

where the point sources and the diffuse radiation have been convolved with the beam. In our application, we are interested in extracting the locations and the intensities of the point sources. We thus assume that the intensities of the point sources are sufficiently above the level of the rest of the signal, and consider the latter as just a disturbance superimposed to the useful signal. If $c(x, y)$ is the signal which does not come from the point sources, model (1) becomes

$$d(x, y) = \sum_{\alpha=1}^{n} a_\alpha \, b(x - x_\alpha, y - y_\alpha) + c(x, y). \tag{2}$$

If our data set is a discrete map of N pixels, the above equation can easily be rewritten in vector form, by letting d be the lexicographically ordered version of the discrete

map $d(x, y)$, a be the n-vector containing the positive source intensities a_α, c the lexicographically ordered version of the discrete map, $c(x, y)$, and ϕ be an $N \times n$ matrix whose columns are the lexicographically ordered versions of n replicas of the map $b(x, y)$, each shifted on one of the source locations. Equation (2) thus becomes

$$d = \phi\, a + c. \tag{3}$$

Looking at Eqs. (2) and (3), we see that, if the goal is to find locations and intensities of the point sources, our unknowns are the number n, the list of locations (x_α, y_α), with $\alpha = 1, \ldots n$ and the vector a. It is apparent that, once n and (x_α, y_α) are known, matrix ϕ is perfectly determined. Let us then denote the list of source locations by the $n \times 2$ matrix R, containing all their coordinates. For the CMB we can assume that c is a Gaussian random field with zero mean and known covariance ξ. Thus the likelihood function is

$$p(d|n, R, a) = \exp\left(-(d - \phi\, a)^t \xi^{-1} (d - \phi\, a)/2\right). \tag{4}$$

If we define $M = \phi^t \xi^{-1} \phi$, $e = \phi^t \xi^{-1}\, d$, the maximization of (4) leads us to the linear system

$$Ma = e \tag{5}$$

where M is a $n \times n$ matrix. The solution of this system will yield the maximum likelihood estimator of the source intensities.

One problem with this approach is that, in principle, we know neither the number n of point sources nor their positions. One standard way of dealing with this difficulty is considering in (5) the local maxima of e and selecting as source positions these local maxima above a certain threshold. A 5σ or 4σ threshold, with σ the standard deviation of e, are typically used, since such high fluctuations rarely have their origin in the CMB or the noise.

Finally, we have to find suitable methods to solve the system shown in (5), taking into account that the number of sources can range from several to thousands depending on the size of the region studied and also on the frequency analyzed.

The problem statement, as described above, involves the processing of large matrices, if we want to cover a significant region of space. This can lead to excessive computation times as well as loss of precision. In this work, we provide an efficient solution with both aspects in mind: to get a reasonable run time and a numerically stable algorithm. To achieve both objectives, we resorted to the use of parallel computing and high performance numerical libraries.

3 Efficient implementations

First, it should be noted that when we are building the system $Ma = e$ we consider that the matrices M, ϕ and ξ are of order N, while the vectors e and d have N rows. Once vector e has been filtered by using the fixed threshold, matrix ϕ is set to $N \times n$

by choosing the adequate rows. Using the same notation as in [7], the matrices ϕ and ξ can be generated from: the number of pixels (N), the pixel size (PIX) and the full width half maximum of the beam ($FWHM$).

To solve the system (5) is necessary to calculate the matrix $M = \phi^t \xi^{-1} \phi$, and the vector $e = \phi^t \xi^{-1} d$, this should be done as efficiently as possible. A classical approach could start by computing the inverse of ξ (see [7]) as the means for calculating the vector e and the matrix M. Then, after applying a threshold process, the linear system $Ma = e$ can be solved. The computational cost of the classical approach implies $2N^3 + 2N^2 + 6Nn$ Flops. The cost of generating the matrices ϕ and ξ must be added to the previous one.

However, from the numerical point of view, it should be desirable to obtain M and e without calculating the inverse of ξ. Some other ideas should be used in order to obtain an efficient algorithm. We have applied the following ones:

- Avoid unstable operations like computing inverses or multiplying large matrices. Instead use orthogonal transformations if possible.
- Try to solve large scale problems, having in mind this:
  - Use moderately the memory, avoiding unnecessary storage of data.
  - Get a moderate execution time.
- Organize the algorithms in such a way that high performance sequential or parallel libraries can be used.

With these ideas an efficient algorithm can be derived. As $\xi \in R^{N \times N}$ is a symmetric positive definite matrix, Cholesky decomposition can be used to obtain a lower triangular matrix L such that: $\xi = LL^t$ ([13]). Hence, vector e can be expressed as:

$$e = \phi^t \xi^{-1} d = \phi^t L^{-t} L^{-1} d = \phi^t L^{-t} c_1 = \phi^t c_2 \tag{6}$$

with $c_1 = L^{-1} d$ and $c_2 = L^{-t} c_1$.

Thus, vector e can be computed by performing a matrix-vector product, where matrix $\phi \in R^{N \times N}$. Observe that these operations involve a cost of $(N^3)/6 + 4(N^2)$ Flops.

As explained in the previous section, thresholding can be applied now to vector e, obtaining those positions with a value higher than 4σ. This is equivalent to obtain a selection matrix $P \in R^{N \times n}$, which consists of those columns of the identity matrix with a '1' in the position determined by the thresholding of vector e, and obtain $\tilde{e} = P^t e = (\phi P)^t c_2$.

Now, in order to construct the part of matrix M which is involved in the threshold linear system, we construct

$$\tilde{M} = P^t M P = (\phi P)^t \xi^{-1} (\phi P) = \tilde{\phi}^t L^{-t} L^{-1} \tilde{\phi}, \tag{7}$$

with $\tilde{\phi} = \phi P \in R^{N \times n}$.

Thus, $\tilde{M} = (L^{-1}\tilde{\phi})^t (L^{-1}\tilde{\phi}) = Z^t Z$, with $Z = L^{-1}\tilde{\phi}$. If we compute the QR decomposition of $Z = QR$, with $Q \in R^{N \times N}$, orthogonal, and $R \in R^{N \times n}$, upper triangular, $\tilde{M} = Z^t Z = (QR)^t (QR) = R^t R$ and linear system $Ma = e$ can be

expressed as $(R^t R)a = \tilde{\phi}^t c_2$. Thus, vector a can be computed by solving the triangular linear systems $R^t y = \tilde{\phi}^t c_2$ and $Ra = y$.

The construction of $\tilde{M}$ involves $(N^2)n + 2n^2(N - n/3)$ Flops and the solution of the final linear systems involves $2n^2$ Flops.

These ideas can be summarized in the following algorithm:

Algorithm CMB

Input N, PIX, $FWHM$, $d \in R^{N\times 1}$

Step 1. Generate matrices ϕ and ξ
Step 2. Compute $\xi = LL^t$ (Cholesky factorization)
Step 3. Obtain e:
  Solve $L * c_1 = d$ and $L^t c_2 = c_1$
  Compute $e = \phi^t c_2$
Step 4. Calculate the positions of e that are above the threshold $(e(i) \geq 4\sigma, e \rightarrow \tilde{e})$
Step 5. Get the columns of ϕ associated with the indices from Step 3: $\phi \rightarrow \tilde{\phi}$
Step 6. Solve $LZ = \tilde{\phi}$
Step 7. Compute the QR factorization of Z $(Z = QR)$
Step 8. Solve the triangular systems: $R^t y = \tilde{e}$, $Ra = y$

Output a

Finally, it should be noted that considering the high number of data and operations involved in the resolution of the problem, the use of parallel strategies is particularly suitable.

4 Implementation details and experimental results

We have implemented the two algorithms described in the previous section: We call *Classical Algorithm* to the one that constructs the matrix M and the vector e starting from the inverse of ξ. In turn, the *CMB Algorithm* avoids the inverse computation and uses matrix decomposition techniques.

In both algorithms, OpenMP ([8]) is used when possible. OpenMP is an API that supports multi-platform shared memory multiprocessing programming techniques on most processor architectures and operating systems. Besides, arithmetic intensive operations of the algorithms have been addressed through calls to the appropriate subroutines of LAPACK [6], i.e. Cholesky factorization with *DPOTRF*, QR factorization with *DGEQRF* and so on.

The testbed system used in the experimentation is composed by one Intel Xeon E5530 Quad-Core processors (4 cores) running at 2.40 GHz with Ubuntu Linux distro (10.04.2 LTS) as operating system. The high performance implementation of LAPACK was provided by Intel MKL (*Mathematical Kernel Library*, version 10.3). Finally, experiments reported in this section employ IEEE 754 double precision arithmetic.

Coming back to the algorithm described in Sect. 3, we can observe an initial step which is the same as for the Classical: Step 1. Generate matrices ϕ and ξ. Despite this step can be considered as an initialization step, it is computationally an important step as we can see in Table 1.

Table 1 Time (s) of an initial implementation of the algorithm described in Sect. 3 when $N = 2^{14}$ and standard values of PIX, $FWHM$ and d are used

Step/cores	1	4
Step 1	$3.36e+03$	$1.47e+03$
Step 2	$1.49e+02$	$3.86e+01$
Step 3	$4.30e-01$	$2.79e-01$
Step 4	$1.73e-04$	$1.79e-04$
Step 5	$2.48e-03$	$2.54e-03$
Step 6	$1.47e+00$	$8.72e-01$
Step 7	$2.27e-02$	$1.61e-02$
Step 8	$4.01e-05$	$4.70e-05$

However, the matrices ϕ and ξ that appear in the problem are symmetric Toeplitz-block Toeplitz matrices with symmetric blocks. A block matriz A whose (i, j)th block A_{ij} is a function of $(i - j)$ is called block Topelitz matrix (see [23]). When A_{ij} is itself a Toeplitz matrix, A is called Toeplitz-block Toeplitz matrix. Using the features provided for this structure we have obtained an efficient algorithm that greatly reduces the computational cost of the algorithm describes in Sect. 3.

Figure 1 shows the execution times obtained for the algorithms considered. It shows that the calculated times are much higher for the Classical algorithm. For example, if N is equal to 2^{14} (16,384) the time of the Classical algorithm is more than 47 times that of the CMB algorithm when the number of cores is greater than one (these results can also be seen in Table 2).

The time of CMB algorithm is small. This suggests the possibility of studying wider regions of space which involves the processing of larger matrices at an affordable execution time by using a larger number of cores. In addition, the technique used in the CMB algorithm is an efficient alternative that can be also applied in more complex computational methods such as Bayesian methods proposed in [7].

5 Simulations

In order to check the performance of the new method, we have carried out several simulations resembling the observational data collected by the LFI of the Planck satellite.

We have simulated data with the characteristics of the 30 GHz channel of the Planck satellite. Our simulations are flat patches of $N = 128 \times 128$ pixels, so that the size of each patch is 14.66×14.66 degrees. Each simulated patch consists of several components: a map of point sources, distributed in flux according to the De Zotti counts model, (see [10]), a CMB map generated by using the power spectrum which produces the best fit to the WMAP 5-year maps, (see [16]) and the instrumental noise.

The CMB map and the point source map are added and convolved with the observational beam, finally the noise is included to create the final input map. If we use the terminology of Sect. 2, d is the final map, in vector form, a_α means the point source fluxes in the point source map, b is the beam pattern and c the noise plus CMB, i.e the contamination which hampers our detection of the sources. But for the Galactic foregrounds, which we do not include in our simulations for the sake of simplicity, we have considered the relevant components of the observational data.

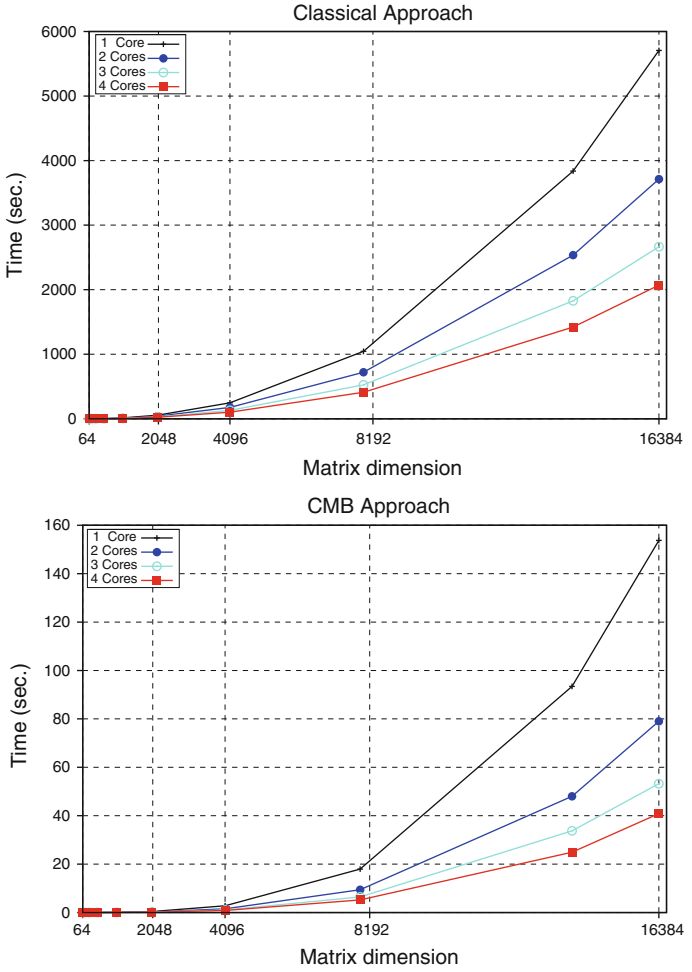

Fig. 1 Execution time for the classical and CMB algorithms

Table 2 Time (s) for $N = 2^{14}$

Algorithm/cores	1	2	3	4
Classical	$5.71e+03$	$3.71e+03$	$2.67e+03$	$2.07e+03$
CMB	$1.54e+02$	$7.90e+01$	$5.32e+01$	$4.09e+01$

In order to solve our problem, we also need to know the matrix ϕ, an $N \times N$ matrix which incorporates the information about the observational beam, and the covariance matrix ξ, which is computed by using the power spectrum of the WMAP 5-year maps, (see [16]). Since we can compute both matrices, we have all the elements to solve our problem in an efficient way.

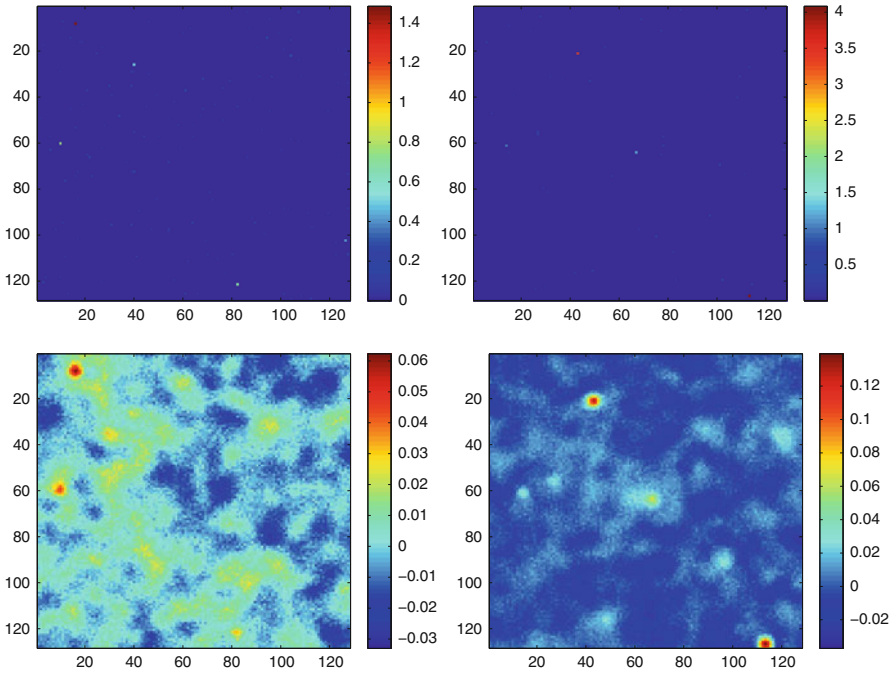

Fig. 2 This figure shows two simulations at 30 GHz. In the *upper panel* simulations of point sources and in the lower the same simulations including the CMB plus noise

In the following, we comment the results of two of our simulations (see Fig. 2), which are representative of the performance of the method. In our first simulation, when we use a 4σ threshold for e, we are able to detect 2 point sources in our map. The first one has a detected flux of 1.25 Jy[2] and is found in the pixel (8,16) of the image. Its real position is (8,16) and its real flux is 1.49 Jy. The second source is detected at (59,10) with a flux of 1.13 Jy. Its real flux is 0.75 Jy and its real position (60,10). Similar results are obtained with the classical method, but with a slower and less efficient technique. Note that the positions are recovered very well and the fluxes with an error due not to the computational method but to the random character of the CMB and the noise: we do not know the particular values of the contamination at each pixel, just the statistical properties of noise and CMB, both are Gaussian random fields with known covariance and we exploit this knowledge by using a maximum likelihood estimator, as explained in Sect. 2.

In our second simulation, we detect above a 4σ level three sources with detected fluxes 3.75, 3.45 and 1.34 Jy respectively. Their real fluxes are 4.08, 3.31 and 1.19 Jy. In this case, the sources are detected in their real positions.

We have thus checked that our technique has a good performance, with regard to the position determination and the flux estimation of the sources.

[2] The Jansky, Jy, is the standard unit of flux in Radioastronomy. 1 Jy $= 10^{-26}$W/(m^{2}Hz).

6 Concluding remarks

We have proposed an efficient algorithm, with a high degree of parallelism that can replace advantageously the classical approaches.

As main advantages of algorithm CMB we can cite:

- It allows to confront large scale problems with a reasonable execution time, optimizing the memory usage.
- Its parallelization is very efficient; near-optimal speedups have been obtained in many cases.
- The constructed algorithm is scalable in the sense that execution time can be maintained, by increasing the problem size and the number of cores at the same rate.
- The use of high-performance libraries and the organization of the algorithm guarantees numerical stability and portability.
- Techniques developed can also be applied to the resolution of Bayesian methods described in [7], thus completing an important analysis tool.
- As explained in Sect. 5, we have used our new method to detect point sources in simulated CMB maps. These maps resemble the real ones surveyed by the LFI (Planck satellite). The new technique allows us to find the simulated point sources in their positions and to estimate their corresponding fluxes. This can be done in a very efficient and fast way. It would be very interesting to explore in the future the application of the method to more complex detection strategies, such as Bayesian techniques.
- An accurate detection and flux determination of point sources is an essential step in the study of the CMB fluctuations. These fluctuations are fundamental data to calculate the cosmological parameters and also to study the chemistry of the early Universe.

Acknowledgments This work was financially supported by the Spanish Ministerio de Ciencia e Innovación and by FEDER (Projects TIN2010-14971, TIN2008-06570-C04-02, TEC2009-13741 and CAPAP-H3 TIN2010-12011-E), Universitat Politècnica de València through Programa de Apoyo a la Investigación y Desarrollo (PAID-05-10) and Generalitat Valenciana through project PROMETEO/2009/013. We thank Diego Herranz for his help with the CMB simulations.

References

1. P.A.R. Ade et al., Planck early results: the Planck mission. Astron. Astrophys. (2011, in press)
2. P. Alonso, R. Cortina, I. Díaz, J. Ranilla, Blocking Neville elimination algorithm for exploiting cache memories. Appl. Math. Comput. **209**, 2 (2009)
3. P. Alonso, R. Cortina, F.J. Martínez-Zaldívar, J. Ranilla, Neville elimination on multi- and many-core systems: OpenMP, MPI and CUDA. J. Supercomput. **58**, 215 (2011)
4. P. Alonso, R. Cortina, E.S. Quintana-Ortí, J. Ranilla, Increasing data locality and introducing level-3 BLAS in the Neville elimination. Appl. Math. Comput. **218**, 3348 (2011)
5. P. Alonso, R. Cortina, J. Ranilla, A.M. Vidal, An efficient and scalable block parallel algorithm of Neville elimination as a tool for the CMB maps problem. J. Math. Chem. doi:10.1007/s10910-010-9769-0
6. E. Anderson et al., *LAPACK Users' Guide* (Society for Industrial and Applied Mathematics, Philadelphia, 1999)
7. F. Argüeso et al., A Bayesian technique for the detection of points sources in cosmic microwave background maps. Mon. Not. R. Astron. Soc. **414**, 410 (2011)

8. B. Chapman, G. Jost, R. van der Paas, *Using OpenMP: Portable Shared Memory Parallel Programming* (The MIT Press, Cambridge, 2008)
9. C.J. Cramer, *Essentials of Computational Chemistry: Theories and Models* (Wiley, England, 2004)
10. G. De Zotti et al., Predictions for high-frequency radio surveys of extragalactic sources. Astron. Astrophys. **431**, 893 (2005)
11. V.K. Dubrovich, Blurring of spatial microwave fluctuations by molecular last scattering. Astron. Lett. J. Astron. Space Astrophys. **19**, 53 (1993)
12. M. Gasca, C.A. Michelli, *Total Positivity and its Applications* (Kluwer Acad. Publ., Dordrecht, 1996)
13. G.H. Golub, C.F. Van Loan, *Matrix Computations* (Johns Hopkins University Press, Baltimore, 1996)
14. M. Lopez-Caniego et al., Comparison of filters for the detection of point sources in Planck simulations. Mon. Not. R. Astron. Soc. **370**, 2047 (2006)
15. R. Maoli, F. Melchiorri, D. Tosti, Molecules in the postrecombination Universe and microwave background anisotropies. Astrophys. J. **425**, 372 (1994)
16. M.R. Nolta et al., Five-year wilkinson microwave anisotropy probe (WMAP) observations: angular power spectrum. Astrophys. J. Suppl. **180**, 296 (2009)
17. A.A. Penzias, R.W. Wilson, A measurement of excess antenna temperature at 4,080 Mc/s. Astrophys. J. **142**, 419 (1965)
18. D.R.G. Schleicher et al., Effects of primordial chemistry on the cosmic microwave background. Astron. Astrophys. **490**, 521 (2008)
19. G. Smoot et al., Structure in the COBE differential microwave radiometer first-year maps. Astrophys. J. **396**, L1 (1992)
20. D.N. Spergel et al., First-year wilkinson microwave anisotropy probe (WMAP) observations: determination of cosmological parameters. Astrophys. J. Suppl. **148**, 175 (2003)
21. J.A. Tauber, The Planck mission. in *New Cosmological Data and the Values of the Fundamental Parameters, Proceedings of IAU Symposium*, vol. 201, ed. by A. Lasenby, A. Wilkinson (2005), p. 86.
22. L. Toffolatti et al., Extragalactic source counts and contributions to the anisotropies of the cosmic microwave background: predictions for the Planck Surveyor mission. Mon. Not. R. Astron. Soc. **297**, 117 (1998)
23. M. Wax, T. Kailath, Efficient inversion of Toeplitz-block Toeplitz matrix. IEEE Trans. Acoust. Speech **31**, 5 (1983)